

PVA-Based Nanofibers Containing Chitosan Modified with Graphene Oxide and Carbon Quantum Dot-Doped TiO₂ Enhance Wound Healing in a Rat Model

Original

PVA-Based Nanofibers Containing Chitosan Modified with Graphene Oxide and Carbon Quantum Dot-Doped TiO₂ Enhance Wound Healing in a Rat Model / Norouzi, F.; Pourmadadi, M.; Yazdian, F.; Khoshmaram, K.; Mohammadnejad, J.; Sanati, M. H.; Chogan, F.; Rahdar, A.; Bairo, F.. - In: JOURNAL OF FUNCTIONAL BIOMATERIALS. - ISSN 2079-4983. - ELETTRONICO. - 13:4(2022), p. 300. [10.3390/jfb13040300]

Availability:

This version is available at: 11583/2977772 since: 2023-04-05T14:31:55Z

Publisher:

MDPI

Published

DOI:10.3390/jfb13040300

Terms of use:

This article is made available under terms and conditions as specified in the corresponding bibliographic description in the repository

Publisher copyright

(Article begins on next page)

Optimal Throughput Management in UAV-based Networks during Disasters

Luca Chiaraviglio,^(1,2) Lavinia Amorosi,³ Francesco Malandrino,⁴ Carla Fabiana Chiasserini,⁵
Paolo Dell’Olmo,³ Claudio Casetti⁵

- 1) EE Department, University of Rome Tor Vergata, Italy, email: luca.chiaraviglio@uniroma2.it
- 2) Consorzio Nazionale Interuniversitario per le Telecomunicazioni (CNIT), Italy
- 3) DSS Department, University of Rome Sapienza, Italy, email {name.surname}@uniroma1.it
- 4) IEIIT, National Research Council of Italy, Turin, Italy, email francesco.malandrino@ieiit.cnr.it
- 5) DET Department, Politecnico di Torino, Italy, email {name.surname}@polito.it

Abstract—Small Cells (SCs) installed on board of Unmanned Aerial Vehicles (UAVs) are a promising solution to provide wireless coverage to users escaping from an area affected by a disaster event. In this paper, we target the problem of maximizing the throughput over a set of areas in a disaster-affected territory. More in depth, we take into account: i) the limited capacity of the UAV-SC battery, ii) the maximum throughput that can be managed by each UAV-SC (due to backhauling/processing constraints), iii) the number of UAV-SCs that can simultaneously cover the same area. We then formulate the MT-UAV problem, which is able to schedule the UAV-SC missions over a set of Time Slots (TSs) to maximize the total area throughput. Results, obtained over a realistic scenario, reveal that the total throughput is clearly impacted by the UAV-SC backhauling/processing constraints, rather than the number of UAV-SCs providing coverage over the same area. Moreover, we analyze the UAV-SC missions selected by MT-UAV, showing that a typical mission is performed over multiple consecutive TSs. Therefore, we claim that the UAV-SC battery capacity is fundamental to guarantee sufficiently long missions to satisfy the throughput requirements over multiple TSs.

Index Terms— emergency networks, UAV mission planning, optimization, performance evaluation

I. INTRODUCTION

Providing wireless connectivity in the immediate moments after a disaster event is a key feature to improve rescue operations as well as to provide information to the people that are escaping from the affected area [1], [2]. In this scenario, the traditional cellular network may be (not fully) available, due to a variety of failure types, which include, e.g., electricity faults, tower damages, fiber cuts, etc. Consequently, large portions of territory in a disaster area experience a complete lack of network coverage. To face this issue, Small Cells (SCs) mounted on top of Unmanned Aerial Vehicles (UAVs) are a promising solution to bring radio resources in the zones affected by the disaster [3], [4]. Compared to the traditional cellular network, which typically requires a large amount of time to be fully restored, UAV-SCs guarantee a fast reactivation of connectivity, as soon as they reach the affected areas [5].

Traditionally, the exploitation of UAVs in disaster areas has been advocated by a variety of works (see, e.g., [6], [7], [8], [9], [10]). The tasks demanded to UAVs include disaster assessment [6], surveillance [7], imagery collection [8], video recording [9], and standalone communication system [10]. More in depth, typical problems that emerge when UAV-SCs are used to provide connectivity include placement optimization [11], throughput-coverage optimization [5], team coordination [12] and mission scheduling [13].

In this paper, we face the problem of maximizing the throughput to a set of users in a disaster area, by taking into account the following key features: i) the limited battery capacity of each UAV-SC, ii) the maximum data rate that can be managed by the UAV-SC (due to limited backhauling and/or processing capabilities), iii) the radio features implemented on the UAV-SCs. Specifically, we target the following questions: Is it possible to maximize the users throughput in a disaster area by properly scheduling the UAV-SCs missions in the 3D space and time? What is the impact of the backhauling and computing constraints? How do the radio capabilities affect the service offered to users? The goal of this paper is to shed light on the aforementioned issues. More in depth, we develop an optimization framework, called MT-UAV, which is able to: i) model the UAV-SCs missions in terms of actions that are set and positions that are visited, ii) schedule the missions by exploiting a multi-period graph, iii) ensuring an admissible battery level, iv) maximizing the throughput offered to users, v) considering different constraints in terms of backhauling/computing and radio capabilities. To the best of our knowledge, none of previous works has conducted a similar analysis. Actually, the closest paper to our work is [14], in which the authors propose an optimization model to plan the UAV-SCs activities in a disaster area. In contrast to them, in this work we go three steps further by: i) including a detailed energy consumption model for the UAV-SCs, ii) introducing a multi-period graph to model the UAV-SCs missions, and iii) evaluating the impact of different backhauling, computing and radio constraints.

Our results, obtained over a realistic case study, clearly demonstrate that the users’ throughput is maximized when

the backhaling/capacity constraint are not too tight (i.e., by allowing a total maximum throughput in the order of dozens of [Mbps] for each UAV-SC). Finally, we investigate the UAV-SCs missions that are selected by our solution, showing that a typical mission involves multiple consecutive TSs. Therefore, we claim that the UAV-SC battery capacity is also a very important aspect to satisfy the throughput requirements.

The rest of the paper is organized as follows. Sec. II reports the problem formulation. Sec. III describes the scenario. Results are analyzed in Sec. IV. Finally, Sec. V concludes our work.

II. PROBLEM FORMULATION

Preliminaries: We assume a set of ground sites providing recharging capabilities to the UAV-SCs. Users are located in a set of areas affected by the disasters. Without loss of generality, we assume that the throughput requests are associated to each area. Moreover, a set of zones, from which the UAV-SCs can cover multiple areas, is provided. In this scenario, a radio link between a ground site and a UAV-SC serving an area has to be established.

We also assume that time is discretized in Time Slots (TSs). In each TS, a UAV-SC can perform one of the following actions: i) recharge at the ground site, ii) staying at the ground site in stand-by mode (and not consuming any energy), iii) moving from a ground site to a zone, iv) serving a subset of areas from a zone, v) hovering over a zone (and not serving any area). Each action in iii)-v) consumes an amount of energy which is precisely modeled in this work.

Focusing then on the capabilities provided by the UAV-SCs, we assume that each UAV-SCs can support up to H_{MAX} [Mbps] traffic from users. Actually, this parameter can be used to constrain the maximum traffic supported in the backhauling radio link, as well as the maximum processing capabilities available on board the UAV-SC. Moreover, we assume that each area can be simultaneously covered by at most Y_{MAX} UAV-SCs.

Sets: Let us denote with A, Z, S, T, U the sets of areas, zones, ground sites, TSs, UAV-SCs, respectively. We then introduce the set of places P as $P = Z \cup S$. We also denote with t_{FIRST} and t_{LAST} the indexes of the first and last TSs, respectively.

In order to model the UAV-SC mission, we introduce a multi-period graph $\mathcal{G} = (N, L)$, where N is the set of nodes, and L is the set of links. Each node $n \in N$ is defined as a pair (p, t) , where $p \in P, t \in T$. Focusing on the set of links L , it is denoted as the union of recharging arcs L^{REC} , staying arcs L^{STAY} , moving arcs L^{MOV} , hovering arcs L^{HOV} , serving arcs L^{SER} , i.e., $L = L^{\text{REC}} \cup L^{\text{STAY}} \cup L^{\text{MOV}} \cup L^{\text{HOV}} \cup L^{\text{SER}}$. Each link $l \in L$ is a possible transition between one node and another one. In particular, a typical link is established from $(p_1, t-1)$ to (p_2, t) . We define the head and the tail of the link as $h(l) = (p_2, t)$ and $t(l) = (p_1, t-1)$, respectively.

In order to enforce the coherence of the UAV-SCs missions, we initially add two fictitious nodes, denoted as Ω and Υ , to the set of nodes N . Moreover, we add to L the set of links

L^Ω and L^Υ , which are defined as $l \in L^\Omega : t(l) = \Omega, h(l) = (p, t_{\text{FIRST}})$ and $l \in L^\Upsilon : t(l) = (p, t_{\text{LAST}}), h(l) = \Upsilon$. In the following step, we associate an unitary token to each UAV-SC. The tokens are injected in Ω , spread over the links L through flow conservation constraints, and collected in Υ . In this way, we enforce the continuity of the UAV-SCs missions throughout the set of TSs, as well as we guarantee that all UAV-SCs are considered by the problem in all TSs. Clearly, we assume that the transitions over the L^Ω and L^Υ links do not consume any energy, and hence the staying state is set in these cases.

Input parameters: Let us denote with $\tau(a, t)$ the throughput requested by area a at TS t . B_{MIN} and B_{MAX} are the minimum and maximum battery levels of a UAV-SC, respectively. H_{MAX} is the maximum total throughput that can be provided by an UAV-SC. Similarly, Y_{MAX} is the maximum number of UAV-SCs that can simultaneously cover the same area.

We denote with $E(l)$ the energy associated to link l in the multi-period graph. The actual values of $E(l)$ are presented in Tab. I and will be analyzed in detail in Sec. III. Intuitively, the value of $E(l)$ depends on the specific places in the head $h(l)$ and the tail $t(l)$, as well as on the specific action activated by l .

Finally, we introduce the compatibility matrix $C(z, a)$ for each zone $z \in Z$ and each area $a \in A$. In particular, $C(z, a) = 1$ area a can be served by an UAV-SC positioned over zone z , 0 otherwise. The rule to set the values of C is based on a maximum distance between a zone and an area, which is set in Sec. III.

Variables: We introduce the continuous variable $\rho(a)$, storing the total throughput provided to an area over the set of TSs. Moreover, $w(z, t)$ is a binary variable set to 1 if there is an UAV-SC in zone z able to serve areas at TS t , 0 otherwise. In addition, $y(a, z, t)$ is a binary variable set to 1 if area a is served by an UAV-SC in zone z at TS t , 0 otherwise. $\phi(a, z, t) \geq 0$ is then a continuous variable storing the fraction of radio resources of UAV-SC in zone z assigned to area a at TS t . We also introduce the binary variable $f(l, u)$, which is set to 1 if UAV-SC u activates link l of the multi-period graph \mathcal{G} , 0 otherwise. Finally, $b(u, t)$ is a continuous variable storing the battery level of UAV-SC u at TS t .

Constraints: We initially impose the flow conservation for each UAV-SC with the following constraint:

$$\sum_{\substack{l \in L: \\ h(l)=(p,t)}} f(l, u) - \sum_{\substack{l \in L: \\ t(l)=(p,t)}} f(l, u) = \begin{cases} 1 & \text{if } (p, t) = \Omega \\ -1 & \text{if } (p, t) = \Upsilon \\ 0 & \text{if } (p, t) \neq \Upsilon, \Omega \end{cases} \quad \forall p \in P, u \in U, t \in T \quad (1)$$

We then activate the variable $w(z, t)$ only if there is at least one UAV-SC in zone z at TS t in serving state. More formally, we have:

$$f(l, u) \leq w(z, t), \quad \forall l \in L^{\text{SER}}, h(l) = (z, t), \quad \forall u \in U, \forall z \in Z, \forall t \in T \quad (2)$$

Moreover, we force $w(z, t)$ to zero if no UAV-SC is in zone z at TS t in serving state:

$$w(z, t) \leq \sum_{u \in U} \sum_{l \in L^{\text{SER}}, h(l)=(z,t)} f(l, u) \quad \forall z \in Z, \forall t \in T \quad (3)$$

In addition, an area a can be served by an UAV-SC in zone z at TS t if and only if there is one UAV-SC (in serving state) in zone z and the value in the compatibility matrix $C(z, a)$ is set to 1. This is ensured by the following constraint:

$$y(a, z, t) \leq C(z, a) \cdot w(z, t), \quad \forall a \in A, z \in Z, t \in T \quad (4)$$

The number of UAV-SCs flying over different zones that can serve a single area a is then bounded by Y_{MAX} . More formally, we have:

$$\sum_{z \in Z} y(a, z, t) \leq Y_{\text{MAX}}, \quad \forall a \in A, t \in T \quad (5)$$

We then impose the fact that an UAV-SC can serve a fraction $\phi(a, z, t)$ of area throughput if and only if the UAV-SC is serving the area:

$$\phi(a, z, t) \leq y(a, z, t), \quad \forall a \in A, z \in Z, t \in T \quad (6)$$

The total amount of throughput provided by the UAV-SC is then bounded by the maximum one H_{MAX} :

$$\sum_{a \in A} \tau(a, t) \cdot \phi(a, z, t) \leq H_{\text{MAX}}, \quad \forall z \in Z, t \in T \quad (7)$$

Moreover, we impose that the each area receives at most the total amount of throughput requested to the network. More formally, we have:

$$\tau(a, t) \cdot \sum_{z \in Z} \phi(a, z, t) \leq \tau(a, t), \quad \forall a \in A, t \in T \quad (8)$$

which is equivalent to:

$$\sum_{z \in Z} \phi(a, z, t) \leq 1, \quad \forall a \in A, t \in T \quad (9)$$

We then compute the total throughput provided to each area as:

$$\rho(a) = \sum_{t \in T} \tau(a, t) \cdot \sum_{z \in Z} \phi(a, z, t), \quad \forall a \in A \quad (10)$$

We then focus on the UAV-SC battery management. We initially impose the UAV-SC battery level constraint:

$$b(u, t) \leq b(u, t-1) + \sum_{\substack{l \in L \setminus L^{\text{STAY}} \\ t(l)=(*,t-1) \\ h(l)=(*,t)}} E(l) \cdot f(l, u) \quad \forall u \in U, t \in T \quad (11)$$

which ensures the computation of UAV-SC battery level as a consequence of the different actions set in the multi-period graph. We consider all the action types except from staying state, which does not consume the UAV-SC battery.



Fig. 1: Areas affected by the flooding from where vehicles escape (red dots), and safe areas vehicles flee to (green dots).

The UAV-SC battery level is then bounded by minimum and maximum values:

$$B_{\text{MAX}} \leq b(u, t) \leq B_{\text{MAX}}, \quad \forall u \in U, t \in T \quad (12)$$

Complete formulation: The overall MAXIMUM THROUGHPUT UAV-SCS (MT-UAV) problem is then defined as:

$$\max \sum_{a \in A} \rho(a) \quad (13)$$

subject to:

- Flow conservation over the multi-period graph: Eq. (1)
- Lower bound on zone serving capabilities: Eq. (2)
- Upper bound on zone serving capabilities: Eq. (3)
- Zone-to-area serving activation: Eq. (4)
- Maximum number of zones serving an area: Eq. (5)
- Fraction of served throughput activation: Eq. (6)
- Maximum served throughput: Eq. (7)
- Total area throughput constraint: Eq. (9)
- Total throughput computation: Eq. (10)
- UAV-SC battery level constraint: Eq. (11)
- Min. and Max. UAV-SC battery levels: Eq. (12)

under variables: $f(l, u) \in \{0, 1\}$, $\forall u \in U, l \in L$, $w(z, t) \in \{0, 1\}$, $\forall z \in Z, t \in T$, $y(a, z, t) \in \{0, 1\}$, $\forall a \in A, z \in Z, t \in T$, $y(a, z, t) \geq 0$, $\forall a \in A, z \in Z, t \in T$, $\rho(a) \geq 0$, $\forall a \in A$, $b(u, t) \geq 0$, $\forall u \in U, t \in T$.

III. DESCRIPTION OF THE SCENARIO

In order to test our approach, we consider the scenario depicted in Figure 1. Red areas therein correspond to areas hit by a disaster, namely, a flooding. Upon receiving an evacuation warning, users located in these areas will try and drive to safer, higher-ground areas, denoted by the green color in Figure 1. More in depth, we simulate the flooding itself through a software called Hazus [19], developed by the American Federal Emergency Management Agency (FEMA). Hazus can simulate multiple types of disasters, including fires, earthquakes, and flooding. Given the scale of the disaster, e.g.,

TABLE I: Breakdown of the links and the energy components in the multi-period graph.

Case	$t(l)$	$h(l)$	Action	Link	Energy Symbol	Energy Value / Energy Terms	Reference / Equations
1	$(s, t-1)$	(s, t)	REC	$l \in L^{\text{REC}}$	E^{REC}	1000 [Wh]	[15]
2	$(s, t-1)$	(s, t)	STAY	$l \in L^{\text{STAY}}$	E^{STAY}	0 [Wh]	-
3	$(s, t-1)$	(a, t)	MOV	$l \in L^{\text{MOV}}$	$-E_{(s,a)}^{\text{MOV}}$	$-[E_F(l) + E_V(l) + E_D(l)]$	[16], [17] / Eq.(14), Eq.(15), Eq.(16)
4	$(a, t-1)$	(s, t)	MOV	$l \in L^{\text{MOV}}$	$-E_{(a,s)}^{\text{MOV}}$	$-[E_F(l) + E_V(l) + E_D(l)]$	[16], [17] / Eq.(14), Eq.(15), Eq.(16)
5	$(a, t-1)$	(a, t)	HOV	$l \in L^{\text{HOV}}$	$-E^{\text{HOV}}$	$-[E_F(l)]$	[16], [17] / Eq.(14)
6	$(a, t-1)$	(a, t)	SER	$l \in L^{\text{SER}}$	$-E^{\text{SER}}$	$-[E_F(l) + E_B(l)]$	[16], [17], [18] / Eq.(14), Eq.(17)
7	Ω	(p, t_{FIRST})	STAY	$l \in L^{\Omega}$	-	0 [Wh]	-
8	(p, t_{LAST})	Υ	STAY	$l \in L^{\Upsilon}$	-	0 [Wh]	-



Fig. 2: Topology of interest: recharging site S (red dot) and zones Z (blue dots). Links identify sites/zones that are sufficiently close for a UAV-SC to fly from one to another in one TS.

the magnitude of an earthquake, Hazus is able to estimate to which extent each part of the topology will be affected by the disaster itself, e.g., which areas will be reached by water in a flooding.

In order to realistically simulate the mobility of escaping users, we leverage an open-source traffic simulator called MATSim [20]. Unlike more popular simulators such as SUMO, MATSim follows a higher-level, *mesoscopic* approach, and works at the level of individual road segments: it provides the number of vehicles in every road segment for every time step, but not the position of vehicles within the segment. Such a level of detail suits our needs, especially since, in urban scenarios, road segments are much smaller than the coverage areas of an UAV-SC.

Using k-means clustering, we divide the topology into 500 areas, forming the set A . We then identify 100 zones, 7 of which also host recharge sites, corresponding to sets Z and S in the system model. For sake of computational complexity, we only consider a part of the scenario, depicted in Fig. 2, including one recharge site (red dot) and a total of 12 zones (blue dots). Lines in Figure 2 correspond to links in L .

Lastly, we set the $\tau(a, z)$ parameters, by following the three-step approach described in [21, Sec. 6], namely:

- 1) we compute the average attenuation between any zone and area, using the ITU-recommended model [22], itself based on the distance between areas and zones;
- 2) we compute the signal-to-noise (SNR) ratio for each

zone-area pair, by assuming for UAV-SCs the same transmission power and frequency of LTE micro-cell, i.e., 30 [dBm] and 1.8 [GHz], respectively;

- 3) we map the SNR values into the amount of data each resource block can transport, leveraging the measurement study [23].

Notice that we compute the SNR instead of the signal-to-noise-and-interference ratio (SINR), which corresponds to neglecting interference from the regular cellular networks – a fair assumption since the very purpose of sending UAV-SCs to an area is to make up for a disabled or damaged cellular network.

We then consider the setting of the remaining input parameters. Focusing on the set of TSs T , we consider a total period of time of 1530 [minutes], with a TS duration $d(t) = 10$ [minutes]. We also set $|U| = 20$. In this way, in fact, the number of UAV-SCs is larger than the number of zones $|Z|$, thus providing continuous coverage of the selected zones, despite the fact that some UAV-SCs need to be recharged when they battery is depleted. Focusing on the UAV-SC battery limits, we set $B_{\text{MIN}}=100$ [Wh] and $B_{\text{MAX}}=1000$ [Wh], in accordance to [15]. Finally, we consider a maximum distance of 1000 [m] between a zone and a served area to compute the compatibility matrix $C(z, a)$.

In the following, we focus on the energy components in the multi-period graph \mathcal{G} . Tab. I reports for each link the head and tail, the action, the link type, the adopted energy symbol, the energy values or the notation of each term of energy, the reference and/or the corresponding equations in the text. Focusing on the UAV energy consumption, we consider the model thoroughly described in [16], [17]. We refer the reader to [16], [17] for the details, while here we report the main intuitions/settings. In brief, the UAV consumes an amount of energy that depends on the following components: i) level flight energy $E_F(l)$; ii) vertical flight energy $E_V(l)$; iii) blade drag profile energy $E_B(l)$. In particular, $E_F(l)$ is expressed as:

$$E_F(l) = \frac{M \cdot G}{\sqrt{2} \delta \cdot \sigma} \frac{1}{\sqrt{V_H^2(l) + \sqrt{V_H^4(l) + \left(\frac{M \cdot G}{\sigma}\right)^2}}} d(t), \quad (14)$$

where M is the weight of the UAV-SC, G is the gravitational acceleration, δ is the air density, σ is the area of the UAV rotor disks, $V_H(l)$ is the horizontal speed, which is computed as: $V_H(l) = \frac{D(p_1, p_2)}{d(t)}$, where $D(p_1, p_2)$ is the distance between p_1

and p_2 . In our case, we set: $M = 12$ [kg] (this value includes the UAV weight plus the SC weight), $G = 9.81$ [m/s²], $\delta = 1.225$ [kg/m³] [16], $\sigma = 3.14$ [m²] (corresponding to UAV rotors of one meter radius), $D(p_1, p_2)$ in accordance to the real positions of zones and the site in Fig. 2. Focusing instead on the vertical flight energy, it is expressed as:

$$E_V(l) = M \cdot G \cdot V_C(l) \cdot d(t), \quad (15)$$

where $V_C(l)$ is the vertical descending/climbing speed. Let us denote with k the cruise altitude. When the UAV-SC is climbing, $V_C(l) = k/d(t)$. On the other hand, when the UAV-SC is descending, $V_C(l) = -k/d(t)$. In our scenario, we set $k = 200$ [m], an altitude which allows serving the users at ground level under Line Of Sight (LOS) conditions. Moreover, we assume that the climbing is allowed between a site and a zone, while the descending is possible from a zone to a site. In addition, we consider also the blade drag profile term $E_B(l)$, which takes into account the UAV physical parameters. More formally, we have:

$$E_D(l) = \frac{1}{8} \lambda \cdot \delta \cdot \sigma \cdot V_H^3(l) \cdot d(t) \quad (16)$$

where λ is the profile drag coefficient, set equal to 0.08 [16]. Finally, we introduce the amount of energy consumed for providing the cellular service by the UAV-SC, which is expressed as:

$$E_B(t) = P_B(t) \cdot d(t) \quad (17)$$

where $P_B(t)$ is the BS power consumption for serving the users, set equal to 200 [W] [18].

IV. RESULTS

We code the MT-UAV formulation in CPLEX (v.12.7.1) and run it over a Dell EMC Poweredge 230 Server with 64 [GB] of RAM and four Intel Xeon E3-1230v6 CPU at 3.5 [GHz].

We initially consider the variation of the maximum throughput H_{MAX} managed by each UAV-SC as well as the maximum number of zones that can cover the same area Y_{MAX} . Fig. 3 reports the results in terms of: i) percentage of served traffic, expressed as $100 \cdot \sum_{a \in A} \rho(a) / \sum_{a \in A} \sum_{t \in T} \tau(a, t)$ (Fig. 3a), ii) total computation time in [s] before obtaining an optimal solution within 1% of MIP gap (Fig. 3b). Focusing on Fig. 3a, three considerations hold in this case. First, the percentage of served traffic strongly depends on the values of H_{MAX} . Second, the requested traffic is fully satisfied when $H_{MAX} \geq 83.3$ [Mbps]. Third, Y_{MAX} has a very limited impact on the percentage of served traffic, except when the backhauling/processing constraint is very tight (i.e., $H_{MAX} = 0.166$ [Mbps]). Focusing instead on the computation times (Fig. 3b), we can note that the solution of the problem generally requires less than 200 [s]. However, there are cases in which the computation time is consistently higher. For example, for very low values of H_{MAX} , the solution of the problem takes nearly 900 [s].

In the following, we compute the cumulative number of UAV-SC actions set by the MT-UAV formulation. Fig. 4

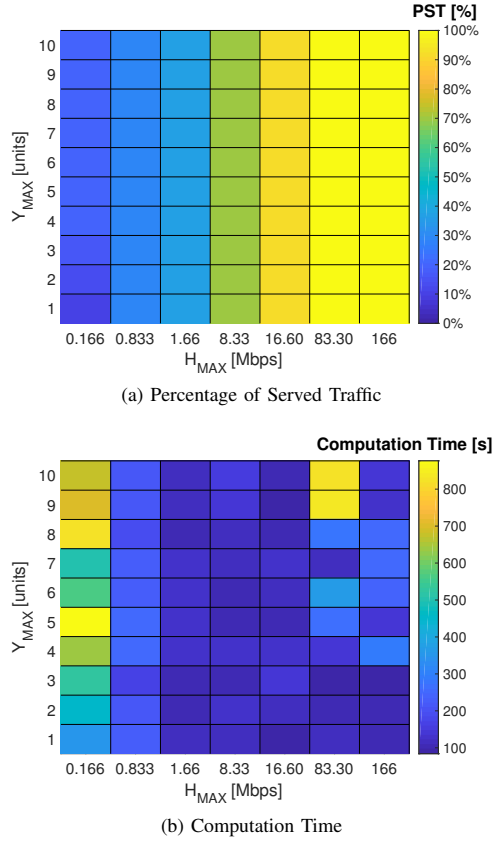


Fig. 3: Percentage of served traffic and computation time vs. the variation of H_{MAX} and Y_{MAX} .

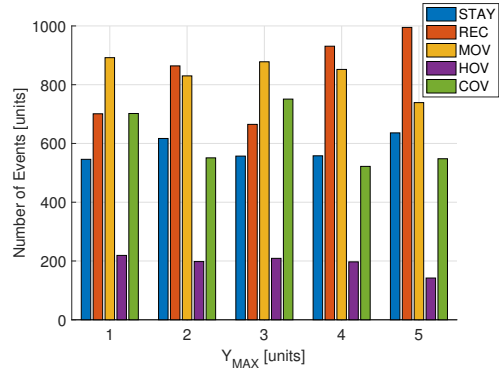


Fig. 4: Actions performed during the UAV-SC missions vs. the variation of Y_{MAX} ($H_{MAX} = 83.30$ [Mbps]).

reports the breakdown of the actions vs. the variation Y_{MAX} , considering $H_{MAX} = 83.30$ [Mbps]. Interestingly, a large amount of actions involve UAV-SC moving, covering, recharging or staying, while the hovering state is less frequently used. Moreover, we can note that this trend is repeated across the different values Y_{MAX} (as expected), due to the fact that the percentage of served traffic is equal to 100% in all these cases, resulting in similar UAV-SC missions.

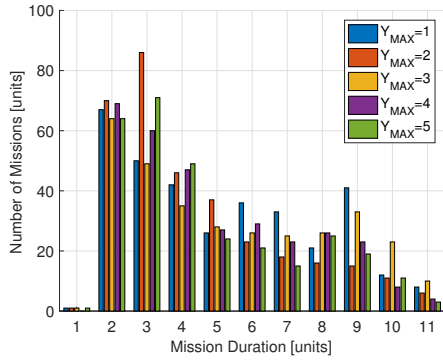


Fig. 5: Histogram of the mission durations (total number of TSs) for different values of Y_{MAX} ($H_{MAX} = 83.30$ [Mbps]).

In the following, we compute the length of each UAV-SC mission, by counting all the consecutive moving/covering/hovering actions between two staying/recharging events. Fig. 5 reports the results, which are again obtained by setting $H_{MAX} = 83.30$ [Mbps] and by varying Y_{MAX} . Although short missions are set (i.e., lasting for 3-4 TSs), it is possible to note that long missions, including up to 11 consecutive TSs, are also exploited. This is another important indication, pointing out that, in a disaster event, the UAV-SC may be required to fly for several consecutive TSs. Consequently, the capacity of the UAV-SCs battery has to be sufficiently large in order to ensure this constraint.

V. CONCLUSIONS AND FUTURE WORKS

We have targeted the problem of managing the throughput requested by a set of areas in a territory affected by a disaster event. To this aim, we have formulated the MT-UAV problem, which is able to maximize the throughput by scheduling the UAV-SC missions over time and space in a multi-period graph. Results, obtained over a realistic scenario, demonstrate that the throughput is clearly maximized only when the backhauling/processing constraint is not too tight (in the order of dozens of Mbps). Moreover, we have shown that the throughput is marginally improved when more than one UAV-SC is allowed to cover the same area. Finally, we have demonstrated that the durations of the UAV-SC missions may be even long, involving multiple TSs to be completed. As next step, we plan a variety of research activities. First of all, the solution of MT-UAV in a more complex scenario is a challenging task, due to the intrinsic intractability of the considered problem. This issue may require e.g., the definition of smart algorithms to efficiently solve the problem in a reasonable amount of time. Secondly, the (possible) scarcity of electricity at the ground site may be faced (e.g., due to power outages that may be incurred even in the areas outside the territory affected by the disaster). Third, we plan to study the possibility to exploit the UAV-SCs to deliver additional services (e.g., energy and/or goods) to the people affected by the disaster.

ACKNOWLEDGMENTS

This work was supported by the University of Rome Tor Vergata BRIGHT project (Mission Sustainability Call).

REFERENCES

- [1] M. Erdelj, M. Król, and E. Natalizio, "Wireless sensor networks and multi-uav systems for natural disaster management," *Computer Networks*, vol. 124, pp. 72–86, 2017.
- [2] M. Erdelj, E. Natalizio, K. R. Chowdhury, and I. F. Akyildiz, "Help from the sky: Leveraging uavs for disaster management," *IEEE Pervasive Computing*, no. 1, pp. 24–32, 2017.
- [3] S. Sekander, H. Tabassum, and E. Hossain, "Multi-tier drone architecture for 5G/B5G cellular networks: Challenges, trends, and prospects," *IEEE Communications Magazine*, vol. 56, no. 3, pp. 96–103, 2018.
- [4] Y. Zeng, R. Zhang, and T. J. Lim, "Wireless communications with unmanned aerial vehicles: opportunities and challenges," *IEEE Communications Magazine*, vol. 54, pp. 36–42, May 2016.
- [5] A. Merwaday, A. Tuncer, A. Kumbhar, and I. Guvenc, "Improved throughput coverage in natural disasters: Unmanned aerial base stations for public-safety communications," *IEEE Vehicular Technology Magazine*, vol. 11, no. 4, pp. 53–60, 2016.
- [6] H. Bendea, P. Boccoardo, S. Dequal, F. Giulio Tonolo, D. Marenchino, and M. Piras, "Low cost uav for post-disaster assessment," *The International Archives of the Photogrammetry, Remote Sensing and Spatial Information Sciences*, vol. 37, no. B8, pp. 1373–1379, 2008.
- [7] I. Maza, F. Caballero, J. Capitán, J. R. Martínez-de Dios, and A. Ollero, "Experimental results in multi-uav coordination for disaster management and civil security applications," *Journal of intelligent & robotic systems*, vol. 61, no. 1–4, pp. 563–585, 2011.
- [8] S. M. Adams and C. J. Friedland, "A survey of unmanned aerial vehicle (uav) usage for imagery collection in disaster research and management," in *9th International Workshop on Remote Sensing for Disaster Response*, p. 8, 2011.
- [9] M. Quaritsch, K. Kruggl, D. Wischounig-Strucl, S. Bhattacharya, M. Shah, and B. Rinner, "Networked uavs as aerial sensor network for disaster management applications," *e & i Elektrotechnik und Informationstechnik*, vol. 127, no. 3, pp. 56–63, 2010.
- [10] M. Erdelj and E. Natalizio, "Uav-assisted disaster management: Applications and open issues," in *Computing, Networking and Communications (ICNC), 2016 International Conference on*, pp. 1–5, IEEE, 2016.
- [11] J. Lyu, Y. Zeng, R. Zhang, and T. J. Lim, "Placement optimization of uav-mounted mobile base stations," *IEEE Communications Letters*, vol. 21, no. 3, pp. 604–607, 2017.
- [12] G. Tuna, B. Nefzi, and G. Conte, "Unmanned aerial vehicle-aided communications system for disaster recovery," *Journal of Network and Computer Applications*, vol. 41, pp. 27–36, 2014.
- [13] A. Trotta, M. Di Felice, F. Montori, K. R. Chowdhury, and L. Bononi, "Joint coverage, connectivity, and charging strategies for distributed uav networks," *IEEE Trans. on Robotics*, vol. 34, no. 4, pp. 883–900, 2018.
- [14] F. Malandrino, C.-F. Chiasserini, C. Casetti, L. Chiaraviglio, and A. Senacheribbe, "Planning uav activities for efficient user coverage in disaster areas," *arXiv preprint arXiv:1811.12450*, 2018.
- [15] L. Amorosi, L. Chiaraviglio, F. D'Andreagiovanni, and N. Blefari-Melazzi, "Energy-efficient mission planning of uavs for 5g coverage in rural zones," in *2018 IEEE International Conference on Environmental Engineering (EE)*, pp. 1–9, IEEE, 2018.
- [16] Y. Sun, D. Xu, D. W. K. Ng, L. Dai, and R. Schober, "Optimal 3d-trajectory design and resource allocation for solar-powered uav communication systems," *arXiv preprint arXiv:1808.00101*, 2018.
- [17] J. M. Seddon and S. Newman, *Basic helicopter aerodynamics*, vol. 40. John Wiley & Sons, 2011.
- [18] "Small cells: No power, no problem." <https://www.isemag.com/2017/09/small-cells-no-power-no-problem/>. Last Accessed: 2019-01-08.
- [19] U.S. FEMA, "Hazardus program." <https://www.fema.gov/hazus>.
- [20] A. Horni, K. Nagel, and K. W. Axhausen, *The multi-agent transport simulation MATSim*. Ubiquity Press London, 2016.
- [21] F. Malandrino, C.-F. Chiasserini, and S. Kirkpatrick, "Cellular network traces towards 5g: Usage, analysis and generation," *IEEE Transactions on Mobile Computing*, 2018.
- [22] ITU, "Recommendation ITU-R P.1411-1."
- [23] FP7 IP EARTH, "Energy efficiency analysis of the reference systems, areas of improvements and target breakdown," 2010.